Journal of Cleaner Production 148 (2017) 23–30

Contents lists available at ScienceDirect

Journal of Cleaner Production

journal homepage: www.elsevier.com/locate/jclepro

Red mud-based geopolymers with tailored alkali diffusion properties and pH buffering ability

Guilherme Ascensão [a, *], Maria Paula Seabra [a], José Barroso Aguiar [b], João António Labrincha [a]

[a] Materials and Ceramic Engineering Department, Aveiro Institute of Materials (CICECO), University of Aveiro, Campus Universitário de Santiago, 3810-193 Aveiro, Portugal
[b] Department of Civil Engineering, University of Minho, Campus de Azurém, 4800-058 Guimarães, Portugal

ARTICLE INFO

Article history:
Received 12 October 2016
Received in revised form
26 January 2017
Accepted 26 January 2017
Available online 30 January 2017

Keywords:
Geopolymer
Red mud
Alkali leaching
pH buffering

ABSTRACT

This study develop novel porous red mud (RM) based geopolymers and evaluates their potential to ensure prolonged pH control. Several properties of the novel geopolymers were examined including buffering ability, alkalis leaching behaviour, mineralogical composition, microstructure and physical properties. Two experimental plans were defined to evaluate the influence of porosity and RM content on those properties. The pH values of the eluted water and geopolymers OH^- ions leaching have been determined over time showing that total OH^- ions and the leaching rate can be tailored by controlling the geopolymers porous structure and the availability of free alkaline species. The lower pH gradient over 28th d (1.64 pH units) was achieved by combining a 0.025 wt% pore forming agent (aluminium powder) with 45 wt% MK replacement by red mud.

A high and prolonged buffer capacity was accomplished, proving that red mud-based geopolymers have potential to be applied as pH buffering material.

1. Introduction

Over the twentieth century the exceptional growth of worldwide population (World Population Prospects, 2015) and of primary energy consumption (Bogomolov et al., 2016) almost led to the exhaustion of certain earth natural resources. In this scenario, the search for renewable and efficient energy sources and sustainable recycling solutions assumed a crucial importance. In 2014, the waste generation in the EU-28 reached 2.5×10^9 t (Eurostat, 2015), and its vast majority still ends in landfills. The development of waste based added-value products targeting novel but large-scale applications, as energy production and wastewater treatment systems, encompasses economic opportunities for distinct actors and will contribute to the faster achievement of a circular economy.

Innovative waste management and upcycling strategies had advanced extremely rapidly in recent years. Waste stream alkaline activation or “geopolymerization” is now deployed on a worldwide commercial scale (Provis et al., 2015) and several types of geopolymeric products has been developed, most of them focused on building industry as Portland cement binder replacement in mortars and concrete. The geopolymers alkaline nature (more than 500 mM free alkaline cations remain in the pore solution (Lloyd et al., 2010)) is a drawback in such building materials, since efflorescences tend to be heavily formed (Škvára et al., 2009). On the other hand, that characteristic might open novel uses, for instance in biogas reactors and wastewaters treatment systems (Bumanis et al., 2015a), where a prolonged alkali diffusion can passively control the pH values. In fact, anaerobic digestion (Taconi et al., 2007) and wastewater treatment efficiency (Wang et al., 2007) is highly dependent on the pH level.

Metakaolin (MK) is the state-of-the-art solid component of geopolymers, but several attempts had been conducted to substitute it. Ashes (Novais et al., 2016a), slags (Pontikes et al., 2013) or vitreous (Novais et al., 2016b) wastes are good candidates, at least as partial substitutes for MK. Bauxite waste (red mud - RM) was also considered by Hairi et al. (2015), due to its highly alkaline nature. Since RM worldwide annual generation surpasses 150×10^6 t (Evans, 2016), several attempts to define viable recycling solutions have been conducted to use of red mud in distinct applications

* Corresponding author.
E-mail address: guilhermeascensao@ua.pt (G. Ascensão).

http://dx.doi.org/10.1016/j.jclepro.2017.01.150
0959-6526/

including: cements (Singh et al., 1996), mortars (Liu and Poon, 2016), geopolymers for structural (Hairi et al., 2015) and insulating applications (Badanoiu et al., 2015), traditional ceramics (Pérez-Villarejo et al., 2012) and in wastewater treatment systems for dyes removal (Hajjaji et al., 2016), metal absorption (Sahu et al., 2016) or catalyst agent (Busto et al., 2016).

In some applications (e.g. common concrete) the admissible incorporation rate is restricted by the sodium concentration. However, for pH buffering the leaching of alkaline species is desirable. The usage waste-based geopolymers as buffering agents is incipient and the production of tailored RM-based geopolymers for such applications remains unexplored. The partial substitution of metakaolin (that requires calcination) for bauxite waste will certainly enhance the environmental footprint of the proposed solution, while at these same time, can constitute a novel environmental remediation strategy for such residue.

Apart from the chemical composition, the fine control of the pore structure is also required in order to control alkali diffusion and pH buffering effect (Ruġele et al., 2014). The transfer of OH^- ions to the surrounding aqueous media will only occur in case of direct surficial contact (Bumanis et al., 2015b), so highly porous geopolymers will promote a more intense alkalis leaching. On the other hand, high initial alkalis leaching rates can result in large pH fluctuations over time and faster exhaustion, which are undesirable for the envisaged applications.

In the present work porous red mud-containing geopolymers were produced using aluminium powder as pore forming agent (Ducman and Korat, 2016). Samples containing distinct contents of red mud and poregene were produced and tested.

2. Experimental

2.1. Materials

Metakaolin (MK) was used as primary source of Al_2O_3 and SiO_2, being purchased under the name of Argical™ from Univar®. The used RM was received from Alcoa Inc., Spain, in the form of a slurry with an average water content of 43 wt%. The RM waste was dried (60 °C), homogenized, milled and sieved at 125 μm.

Geopolymers leaching behaviour depends on the alkali activator nature (Zhuang et al., 2016). The use of NaOH instead of KOH is expected to promote higher buffering performances, since Na^+ ions tend to be weakly bounded to the aluminosilicate framework than K^+ ions. The alkaline activator was a mixture of sodium silicate solution (Quimialmel, Portugal; 13.5 wt% Na_2O; 26.5 wt% SiO_2 and 60.0 wt% H_2O), 10M NaOH solution, and distilled water. The NaOH solution was prepared dissolving 20–40 mesh sodium hydroxide beads (reagent grade, 97%, Sigma Aldrich) in distilled water. The NaOH solution was prepared in advance to allow it to cool down prior to geopolymers preparation.

Commercial aluminum powder with a $D_{50} \cong 50$ μm and a purity degree = 95% (Expandit® BE 1101, GRIMM Metallpulver GmbH, Germany) was used as foaming agent.

2.2. Design of experiments

Two experimental plans were defined to assess the compositional effects and their interaction in the geopolymers properties (Table 1). To evaluate the influence of the pore forming agent, five different formulations were prepared (experimental plan 1, EP1). The amount of aluminum powder ranged between 0.000 and 0.100 wt% (Table 1). Maximum concentration was limited in order to avoid substantial pore coalescence. The second batch of formulations was prepared to assess the influence of RM content (experimental plan 2, EP2). Batch formulations are detailed in Table 1. Fixed molar oxide ($SiO_2/Al_2O_3 = 3.96$; $Na_2O/Al_2O_3 = 1.13$ and $Na_2O/SiO_2 = 0.29$) and solid/liquid (S/L = 0.67) ratios were used.

2.3. Geopolymers preparation

The preparation is described in detail in a previous work (Novais et al., 2016a,b,c,d). In short, it involved: (i) the preparation of the alkaline medium by homogenizing the sodium silicate and NaOH 10M solutions with distilled water at 60 rpm during 300 s; (ii) mixing the dried solid components in a plastic bag for 60 s; (iii) mixing the solid and liquid components mechanically for 600 s at a fixed speed, and (iv) addition of the pore forming agent to the blend and mixing for 120 s at 95 rpm. Then, the slurry was cast into plastic molds and sealed with a plastic film. The samples were cured for 7 d in controlled conditions (40 °C and 65% relative humidity) in a climate chamber (Fitoclima 300 EP10 from Aralab). Afterwards, the samples were demolded and kept at room conditions until the 28th d of curing. According to Zhang et al. (2014), a low curing temperature can have a beneficial impact on the leaching of alkaline species.

2.4. Material and geopolymers characterization

X-ray fluorescence (Philips X'perts PRO MPD spectrometer) was used to determine the chemical composition of the raw materials. Their mineralogical composition was assessed by X-ray diffraction (XRD), conducted on a Rigaku Geigerflex D/max-Series instrument (Cu Kα radiation, 10-80°, 0.02° 2θ step-scan and 10 s/step), and phase identification by X'pert HighScore Plus software.

Laser diffraction analyses (Coulter LS230 analyzer) were employed to determine the particle size distribution of the powered raw materials. Laser diffraction technique (Fraunhofer method) was used for the particles with dimensions between 0.4 μm and 2000 μm whereas Polarization Intensity Differential Scattering (PIDS) was used to particles with lower dimensions (between 0.4 μm and 0.04 μm).

Scanning electron microscopy (SEM - Hitachi S4100) equipped with energy dispersive X-ray spectrometry (EDS, Rontec) was used to evaluated the differences in microstructure of the raw materials and of the produced geopolymers.

Optical analysis was performed in a Leica EZ4HD microscope to analyze the morphological differences between the produced bodies. The samples were cut from cured geopolymers using a Struers Secotom-10 table top cutting machine.

The compressive strength of the 28th d cured geopolymers bodies was determined by using a Universal Testing Machine (Shimadzu model AG-15 TA) operating with a 0.5 mm min^{-1} displacement rate.

Using distilled water as immersion fluid, the Archimedes method was employed to evaluate the geopolymers water absorption capacity, while their bulk density was determined by the relation between the weight and volume of each sample.

The true density of the geopolymer prepared without pore forming agent was measured by helium pycnometer technique using a Multipycnometer, Quantachrome). The total porosity of the prepared geopolymeric bodies was then calculated as suggested by Landi et al. (2013).

The open porosity was determined according the expression:

$$Open\ porosity\ (\%) = \frac{ms - md}{ms - mi} \times 100 \quad (1)$$

where *md* is the dry sample weight, *ms* is the weight of the sample after 24 h immersed in distilled water under vacuum and *mi* is the

Table 1
Experimental plan.

Experimental plan	Formulations	Mixture portion (wt%)					Blowing agent	Solid/liquid wt. ratio
		MK	RM	Na_2SiO_3	NaOH	H_2O	Al	
1	F11	30.00	10.00	53.29	5.71	1.00	–	0.67
	F12	30.00	10.00	53.29	5.71	1.00	0.025	0.67
	F13	30.00	10.00	53.29	5.71	1.00	0.050	0.67
	F14	30.00	10.00	53.29	5.71	1.00	0.075	0.67
	F15	30.00	10.00	53.29	5.71	1.00	0.100	0.67
2	F12	30.00	10.00	53.29	5.71	1.00	0.025	0.67
	F22	26.00	14.00	51.93	3.00	5.07	0.025	0.67
	F23	22.00	18.00	50.50	0.31	9.19	0.025	0.67

hydrostatic soaked weight of each sample.

The experimental error was assessed by testing, for each formulation, three samples (approx. 36 mm of diameter and 60 mm length).

The geopolymers leaching behaviour was determined by the acid-base titration method. Two cubic samples ($2 \times 2 \times 2$ cm) were immersed in 50 mL of distilled water, which was daily renewed. The pH fluctuations of the eluted water in contact with the porous bodies were determined over time (until the 28th d after curing).

The OH^- ions leaching rate was measured by using, as titrant, a HCl solution, and phenolphthalein as acid-base indicator. A 0.035 M HCl solution was employed in the initial 7 d, while a less concentrated (0.0035 M) HCl solution was used on the remaining 21 d. The pH of the eluted water was then determined according to the expression presented by Chauhan (2008).

3. Results and discussion

3.1. Raw materials characterization

The chemical composition of MK and RM are given in Table 2. MK is mostly composed of Al_2O_3 and SiO_2, while RM is mainly constituted by Fe_2O_3. The presence of Al_2O_3, TiO_2 SiO_2 and Na_2O is also significant in the waste.

The XRD patterns of MK and RM are presented in Fig. 1. The MK shows a characteristic pronounced broad hump between 20 and 30° 2θ, indicating a strong amorphous character. Quartz, muscovite and anatase are the crystalline phases identified. By contrast, RM displays sharp hematite peaks and no broad hump was detected. In general these results are in agreement with previous works (Hairi et al., 2015; Badanoiu et al., 2015), despite the expectable variability on the RM chemical composition.

The particle size distribution of the powdered raw materials shows that RM average particle size is finer than MK (Table 3) and its particle distribution is narrow (Fig. 2). RM presents a bi-modal

Table 2
Chemical composition of metakaolin (MK) and red mud (RM).

Oxides (% wt)	MK	RM
SiO_2	54.40	5.67
Al_2O_3	39.40	14.63
Fe_2O_3	1.75	52.25
TiO_2	1.55	9.41
K_2O	1.03	0.08
CaO	0.10	1.88
Na_2O	0.00	4.82
MgO	0.14	0.08
P_2O_5	0.06	0.53
SO_3	0.00	0.32
Cl	0.00	0.02
MnO	0.01	0.06
Loss on ignition	2.66	1.90
Ratio of SiO_2/Al_2O_3	1.38	0.39

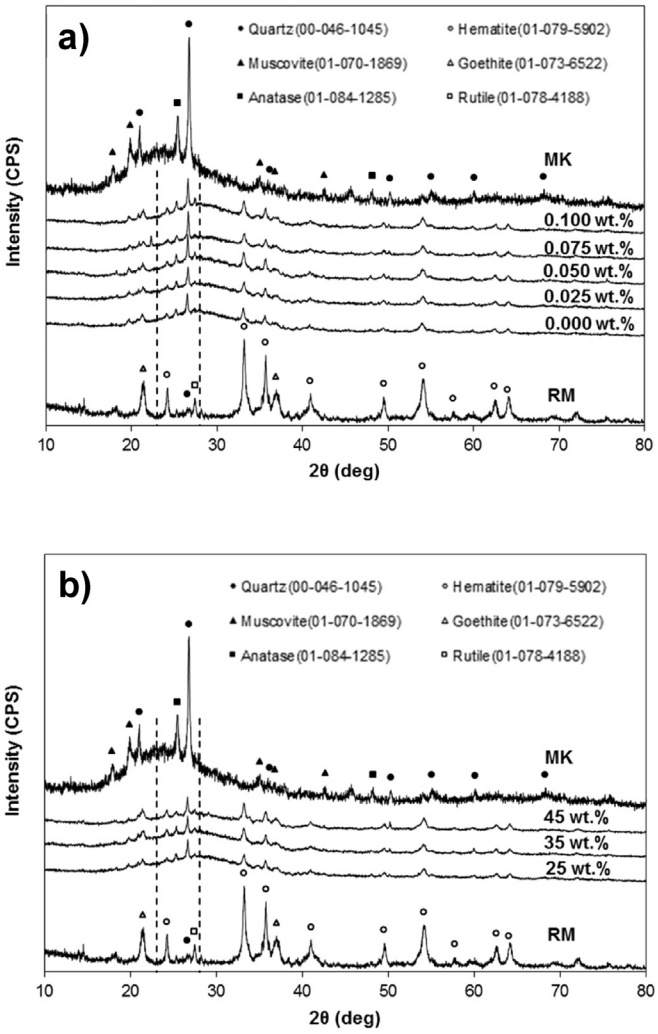

Fig. 1. Representative XRD patterns of the raw materials and geopolymers: **a)** metakaolin (MK), red mud (RM) and geopolymers produced with distinct pore forming agent content; **b)** MK, RM and geopolymers produced with distinct RM contents.

Table 3
MK and RM particle size distribution and average particle size (express in μm).

%<	10	25	50	75	90	Mean
MK	1.15	2.39	4.38	7.49	11.56	5.51
RM	0.32	0.49	0.73	2.22	3.13	1.35

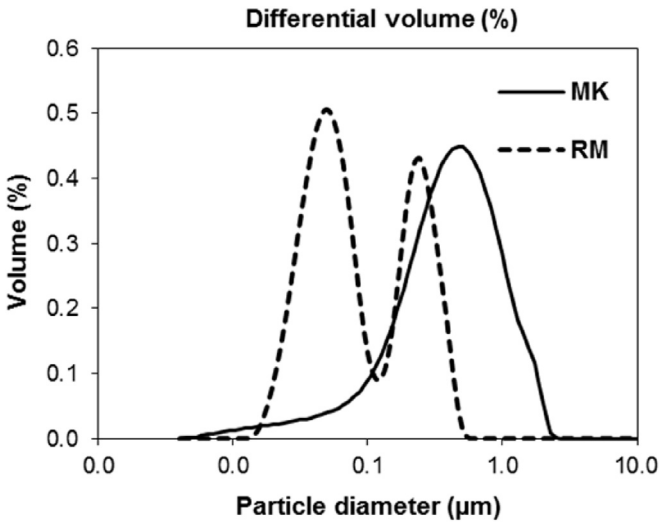

Fig. 2. Particle size distribution of the powered raw materials.

distribution, revealing agglomeration of smaller particles, whereas the size of MK particles is more homogenous. Fig. 3 shows representative SEM micrographs and EDS spectrums of MK (a and c) and of RM (b and d). EDS spectra are in agreement with chemical analyses given in Table 2.

3.2. Geopolymers characterization

3.2.1. Influence of pore forming agent content

X-ray patterns of RM-based geopolymers (cured for 28 d) produced with distinct pore forming agent contents (EP1) are shown in Fig. 1a. The geopolymers show the crystalline peaks of precursor's phases, albeit with reduced intensity. A broad hump between 16 and 39° 2θ is also visible. The centre of this broad hump shifts towards higher 2θ values when compared with MK, revealing the formation of new amorphous phases (Zhang et al., 2012). A geopolymeric gel mainly composed by Si, Al, Fe and Na was formed, which constitutes an additional evidence that geopolymerization reactions took place (Fig. 4). Some unreacted particles were detected, indicating that complete dissolution was not achieved. The crystalline nature of RM contributes to this behaviour, since its dissolution rate will be lower and slower than for MK. The EDS analysis shows that the unreactive particles have variable composition (Fig. 4b), being, however, mainly constituted by the chemical elements detected in RM.

Fig. 5 shows optical and SEM images of geopolymers containing distinct amounts of porogene, after 28 d curing. As expected, the volume and size distribution of pores is greatly affected by the porogene content. As consequence, physical properties such as the density, water absorption and compressive strength of the samples are strongly influenced (see Table 4). The porogene-free sample (F11) presents the highest bulk density (1.34 ± 0.01 g/cm^3), which tends to diminish as the porogene content rises (reduction ranging from 35.8 to 64.4%). It must be mentioned that F11 samples are not physically stable when immersed in water, so they were discarded for further testing. Only its true density (3.30 g/cm^3) was considered to determine the total porosity of the remaining samples.

As expected from the density variations, the porosity and water absorption of the samples increases when the porogene content rises. At the same time the compressive strength decreases. Those relationships are described by 2nd order polynomial equations (fitting over 96.6%), which are not shown here for sake of brevity.

Estimation of the open porosity was only possible for F12 samples, since the others do not submerge in water even after 24 h

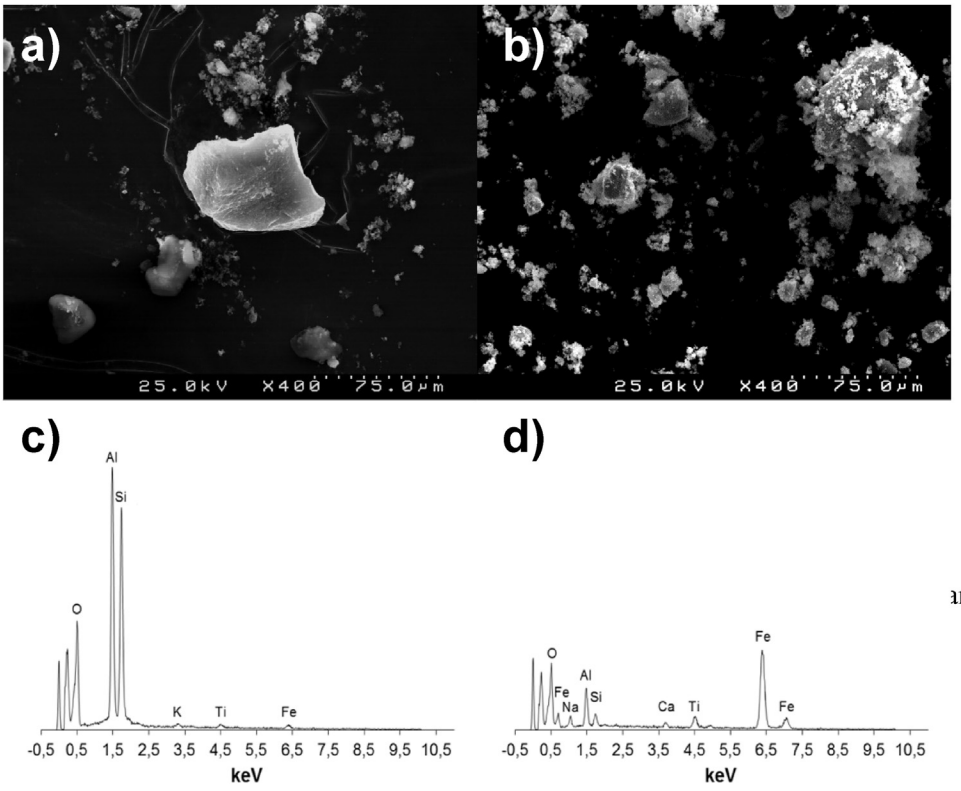

Fig. 3. Representative SEM micrograph and EDS spectrum of metakaolin (**a** and **c**) and red mud (**b** and **d**).

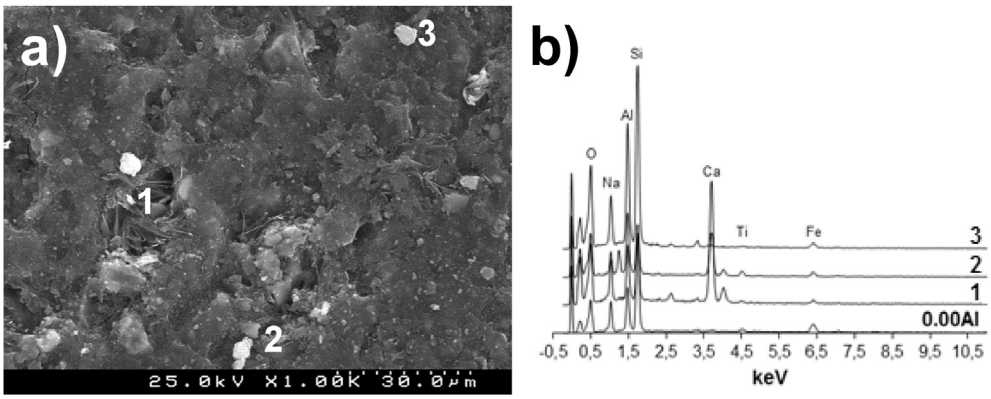

Fig. 4. Representative SEM micrograph (**a**) and EDS spectrum (**b**) of red mud-based geopolymer produced without pore forming agent.

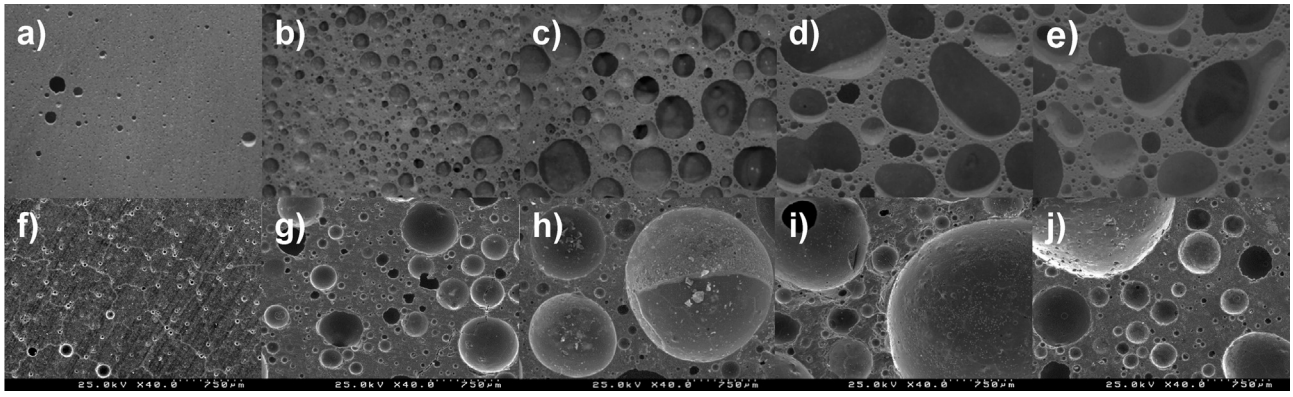

Fig. 5. Optical microscopy (**a**–**e**) and corresponding micrographs (**f**–**l**) of geopolymers containing distinct amounts of pore forming agent, after 28 d of curing: (**a** and **f**) 0.000 wt%, (**b** and **g**) 0.025 wt%, (**c** and **h**) 0.050 wt%, (**d** and **i**) 0.075 wt% and (**e** and **j**) 0.100 wt%.

Table 4
Bulk density, compressive strength, total and open porosity and water absorption of red mud geopolymers samples (cured for 28 d) and corresponding standard deviations.

Experimental plan	Formulations	Bulk density	Total porosity	Open porosity	Closed porosity	Water absorption	Compressive strength
		g/cm^3	%	%	%	%	MPa
1	F11	1.34 ± 0.01	59.52 ± 0.24	–	–	–	–
	F12	0.86 ± 0.02	74.03 ± 0.51	22.49 ± 6.63	51.76 ± 7.28	26.15 ± 0.19	5.84 ± 1.03
	F13	0.63 ± 0.00	81.03 ± 0.11	–	–	29.52 ± 0.60	2.29 ± 0.29
	F14	0.53 ± 0.01	83.89 ± 0.31	–	–	35.34 ± 0.90	1.64 ± 0.68
	F15	0.47 ± 0.02	85.88 ± 0.46	–	–	41.09 ± 4.09	0.70 ± 0.34
2	F12	0.86 ± 0.02	74.03 ± 0.51	22.49 ± 6.63	51.76 ± 7.28	26.15 ± 0.19	5.84 ± 1.03
	F22	0.86 ± 0.01	74.08 ± 0.24	28.28 ± 0.12	45.71 ± 0.16	27.32 ± 0.20	3.73 ± 1.14
	F23	0.87 ± 0.01	73.70 ± 0.16	34.66 ± 0.11	38.94 ± 0.18	33.31 ± 0.21	1.80 ± 0.54

under vacuum. This behaviour suggests that the pores are mostly closed. Nevertheless, a small increase of the open porosity is expected as the aluminium powder rises, as revealed by the slight increase of water absorption values (Table 4). The number, volume and size distribution of the open pores are expected to have a significant role on the alkali diffusion properties (Zhang et al., 2014).

The temporal evolution of pH values of the aqueous solution in contact with geopolymeric bodies is shown in Fig. 6, while the cumulative leaching of OH^- species is presented in Fig. 7. All the produced geopolymers have similar pH buffer capacity in the first 24 h ($\Delta pH = 0.20$), while for longer periods differences become clear. The pH fluctuations are affected by the porosity of the samples, which clearly demonstrate the influence of pore forming agent content on the ability to passively keep high pH values over time (Fig. 8). These results are in agreement with previous findings (Novais et al., 2016c).

The increase of total porosity reduces the bodies' density, resulting in a lower availability of alkaline species per sample. At the same time, as the open porosity rises, the exposed area/volume increases, facilitating the access to its interior. Giannopoulou and Panias (2010) reported that aluminium addition, under constant SiO_2/Na_2O ratio, consume sodium cations as network modifying agents and as negative charge balancing species, which will reduce the leaching of alkaline species.

These combined effects tend to lower pH values and induce more pronounced fluctuations over time as the Al wt% rises. Indeed, the pH gradient over the 28 d of leaching test becomes narrow as the pore forming agent content decreases, ranging from 1.65 to 2.10. Bajare and Bumanis (2014) had reported the behaviour of

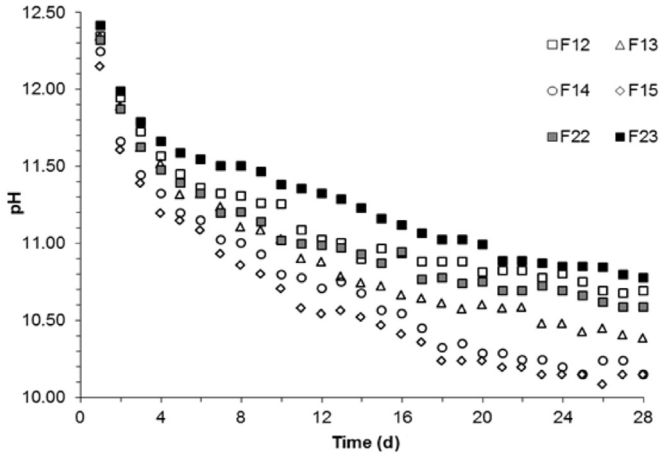

Fig. 6. pH of eluted water solution after 24 h immersion of porous RM based-geopolymers as a function of time.

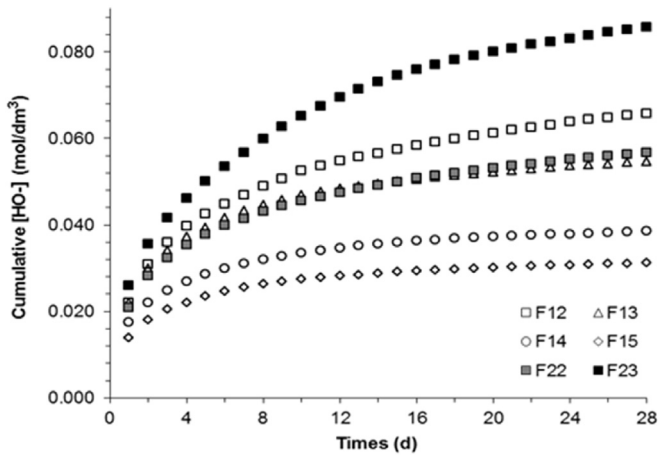

Fig. 7. Cumulative OH^- ions leaching from porous red mud containing geopolymers as a function of time.

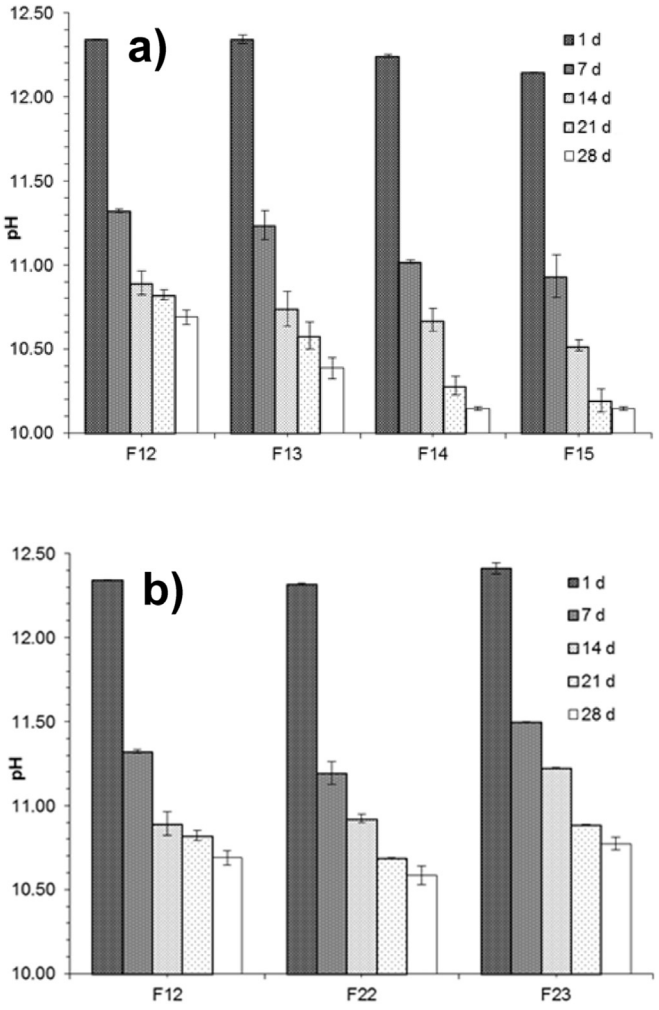

Fig. 8. pH of eluted water solution evolution as a function of time: **a)** EP1-geopolymers produced with distinct Al wt% and **b)** EP2-geopolymers produced with distinct RM wt %.

alkali activated materials produced with NaOH and cured at low temperatures. Those materials show considerable pH fluctuations over time (3.0–5.3 pH units), which are unsuitable for applications were a strict control of pH values is required. The same authors also reported the development of other alkali activated materials with long-term stable leaching properties (pH fluctuation below 1.0 over 25 d of immersion in deionised water). However, their production requires an energy intense synthesis process, which involves a thermal treatment up to 400 °C.

Fly-ash containing geopolymers with prolonged alkalis leaching properties have been reported, being the leaching properties mainly associated to the solid-liquid ratio and to the pore forming agent content (Novais et al., 2016d). The low Na_2O content on the used ashes demand highly concentrated NaOH solutions to increase the total Na_2O concentration, thus assuring high alkali diffusiveness. Through proper compositional design, red mud Na_2O content can mitigate the use of chemicals, which represent 60–80% of geopolymers production cost (Dimas et al., 2009), while kept Na_2O/SiO_2 and Na_2O/Al_2O_3 molar ratios. The influence of solid-liquid ratio on red mud-based geopolymer alkali diffusion properties has not been address in the present investigation but will be reported in future works.

All formulations present an intense OH^- leaching rate in the first few d, with a clear repercussion on the aqueous medium pH (Fig. 7). Afterwards, the OH^- leaching tends to stabilize. After 7 d leached amounts reach 71.3 and 81.7% of the total (Table 5). Intensive initial OH^- leaching rates and high pH values have been reported in the literature by Bajare and Bumanis (2014). The F12 formulation presents the most prolonged OH^- ions leaching profile (Fig. 7) while lower pH fluctuations are also observed over time (Fig. 8a). Nevertheless, the results showed that after the first 4 d of leaching, the pH of eluted water from all formulations lies under an 11.5–10.0 range, which is considered suitable for wastewater chemical clarification (Cheremisinoff, 2002). Still, in order to limit the intensive initial alkali leaching further investigation on compositional effects and/or synthesis conditions is needed.

In anaerobic fermentation processes a considerable initial pH increase is necessary if highly acid subtracts (such as whey) were used by Ruģele et al. (2014), being afterwards active pH control less demanding. The high initial OH^- leach, the long term alkali diffusion properties and the narrow pH fluctuations over time makes the produced red mud-based geopolymers an innovative waste-based material able to act as buffering agent in the envisioned large-scale applications.

Table 5
pH and OH^- leaching values of porous red mud geopolymers after immersion in distilled water.

Experimental plan	Formulations	pH at 1st d	pH at 28th d after leaching test	Leaching of OH^- at 1st d (%)	Cumulative leaching of OH^- at 7th d (%)	Total leaching of OH^- (mol/dm^3)
1	F12	12.34	10.69	33.51	71.28	0.0653
	F13	12.34	10.39	40.35	79.25	0.0544
	F14	12.24	10.15	45.39	80.34	0.0386
	F15	12.15	10.15	44.75	81.66	0.0313
2	F12	12.34	10.69	33.51	71.28	0.0653
	F22	12.32	10.58	36.70	73.08	0.0564
	F23	12.41	10.77	30.20	66.13	0.0851

3.2.2. The influence of RM content

A second experimental plan was design to access the influence of RM content on the geopolymers pH buffering ability. Two additional formulations containing higher amount of RM (35 and 45 wt% of MK replacement) were prepared. The content of pore forming agent and molar oxides and solid/liquid ratios were kept constant (see Table 1). The X-ray patterns of the geopolymers produced with distinct RM contents are shown in Fig. 1b). No significant changes were detected between the samples but the increase of RM content tends to have a negative impact on the reaction extension/rate, due to the higher crystallinity of the waste in comparison to MK. As a consequence, values of the open porosity and water absorption tend to slightly increase with the progress of RM content (Table 4). The bulk density and total porosity of the samples remain similar, which can be attributed to the constant S/L ratio and pore forming agent content. Those compositional parameters seem to govern the mentioned features as reported previously by Novais et al. (2016c).

The optical images and micrographs of the geopolymers (Fig. 9) confirm that the increase of the RM content does not induce significant changes on the number and size of the pores. Within the studied limits the RM content does not exert a strong influence on the density and total porosity of produced materials, and the observed compressive strength reduction (Table 4) can be associated to the lower degree of geopolymerization, which lead to a more fragile geopolymeric structure.

The increase of RM content was expected to enhance the amount of available free alkalis while higher open porosity values are expected to increase their diffusion rate by enlarging the contact area.

Figs. 6 and 7 shows the temporal pH variation of the solution in contact with the bodies, and the OH^- cumulative leaching, respectively. Values of these two variables are only slightly different, especially between the F12 and F22 formulations. Only the F23 bodies show evident differences, in accordance with the increase of open porosity and expectable higher amount of alkaline (sodium) species (introduced by RM). In fact, the increase of open porosity accelerates the leaching rate but can conduct to a fast stabilization/exhaustion if low amounts of alkaline species are available in the material. However, EP2 bodies show enhanced OH^- leaching over time, resulting in low pH fluctuations (ranging from 1.64 to 1.73) (Fig. 6). F23 geopolymers exhibit an excellent ability to act as pH buffering agents which can be related to the higher total amount of OH^- ions and their gradual release. For the F23 bodies the initial OH^- leaching represents 66.1% of the total, while for other formulations (EP1 and EP2) always surpasses 71.0% (Table 4). Yet, a systematic research is needed to define the optimal open porosity range to restrict the initial OH^- leaching and to promote, even further, a more gradual leaching rate of alkaline species.

These results show that a higher RM content promote an increase of the initial pH value while diminishing the pH range after 28 d, as a result of a slower leaching rate (Fig. 8). Thus, the rise of RM content promotes an improvement of geopolymers long term buffering capacity, which makes conceivable to extend the RM content if proper synthesis conditions (e.g. solid/liquid and molar oxide ratio) and open value porosity were ensured. These subjects will be addressed by the authors in future works.

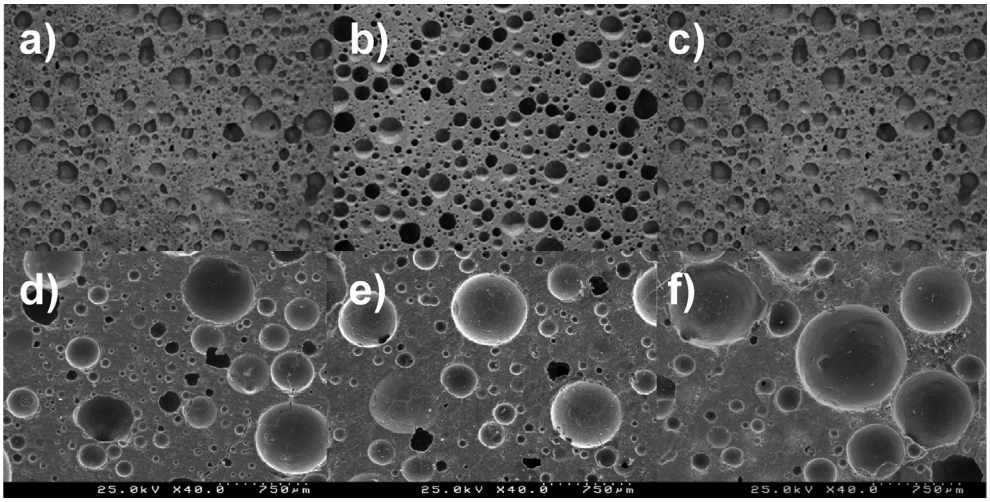

Fig. 9. Optical microscopy (**a**–**c**) and representative micrographs (**d**–**f**) of geopolymers produced using distinct red mud content, after 28 d of curing: (**a** and **d**) 25 wt%, (**b** and **e**) 35 wt% and (**c** and **f**) 45 wt%.

4. Conclusions

In the present work, porous red mud-based geopolymers were synthesized and their pH buffer capacity and temporal alkalis leaching were characterized. The results show that RM-based geopolymers present long term alkali diffusion and pH buffering capability make them potential candidates for applications such as wastewater treatment and in anaerobic digestion for biogas generation. In these, a strict and prolonged control of pH values is required. The influence of RM content and pore forming agent was also evaluated and correlated with the geopolymers microstructure, pH buffering capacity and OH^- leaching rate. The incorporation of red mud (>35 wt%) enhances the leaching rate/extension of alkaline species, due to its own caustic character and to the enlargement of open porosity. The pore forming agent has benefits on the performance only if added in restricted amounts (<0.025 wt %).

The actual red mud-based geopolymers presented lower pH fluctuations (approx. 55.0% less) then glass waste counterparts produced at low temperatures. By contrast, fly-ash containing geopolymers has been reported to show slightly higher buffering performance and lower pH fluctuation over time than our formulations, but its production requires highly concentrated NaOH solutions.

Despite the potential of tested formulations, further research is needed to comprehend the influence of other synthesis parameters (e.g., solid/liquid and molar ratios, pore forming agent type) and to perspective scale-up adaptations for a pilot plant testing.

The produced RM-based geopolymers present interesting features to act as pH buffering agents, being the development of waste based added-value products aligned with the current European environmental policies, which seek the valorization of large-scale industrial wastes, thus reducing landfill disposal practices and contribute to achieve a circular economy.

Acknowledgements

This work was developed within the scope of the project CICECO-Aveiro Institute of Materials, POCI-01-0145-FEDER-007679 (FCT Ref. UID/CTM/50011/2013), financed by national funds through the FCT/MEC and when appropriate co-financed by FEDER under the PT2020 Partnership Agreement.

References

Badanoiu, A.I., Al Saadi, T.H.A., Stoleriu, S., Voicu, G., 2015. Preparation and characterization of foamed geopolymers from waste glass and red mud. Constr. Build. Mater. 84, 284–293.

Bajare, D., Bumanis, G., 2014. Alkali diffusion in porous alkali activated materials. Spectrum 6, 96–110.

Bogomolov, A., Lepri, B., Larcher, R., Antonelli, F., Pianesi, F., Pentland, A., 2016. Energy consumption prediction using people dynamics derived from cellular network data. EPJ Data Sci. 5, 1–15.

Bumanis, G., Rugele, K., Bajare, D., 2015a. The effect of alkaline material particle size on adjustment ability of buffer capacity. Mater. Sci. 21, 405–409.

Bumanis, G., Bajare, D., Dembovska, L., 2015b. Structural investigation of alkali activated clay minerals for application in water treatment systems. Mater. Sci. Eng. 96 (1), 012002.

Busto, R.V., Gonçalves, M., Coelho, L.H.G., 2016. Assessment of the use of red mud as a catalyst for photodegradation of bisphenol A in wastewater treatment. Water Sci. Technol. 74, 1283–1295.

Chauhan, B.S., 2008. Principles of Biochemistry and Biophysics. University Science Press, Laxmi Publications Pvt. Ltd., New Delhi, India.

Cheremisinoff, N.P., 2002. Handbook of Water and Wastewater Treatment Technologies. Butterworth-Heinemann, Woburn, Massachusetts, USA.

Dimas, D., Giannopoulou, I., Panias, D., 2009. Polymerization in sodium silicate solutions: a fundamental process in geopolymerization technology. J. Mater. Sci. 44, 3719–3730.

Ducman, V., Korat, L., 2016. Characterization of geopolymer fly-ash based foams obtained with the addition of Al powder or H_2O_2 as foaming agents. Mater. Charact. 113, 207–213.

Eurostat, 2015. Waste Generation by Economic Activities and Households. European Statistical Data Support, European Commission. ec.europa.eu/eurostat/statistics-explained/index.php/Waste_statistics#Total_waste_generation (Accessed 28 August 2016).

Evans, K., 2016. The history, challenges, and new developments in the management and use of bauxite residue. J. Sustain. Metall. 1, 1–16.

Giannopoulou, I., Panias, D., 2010. Hydrolytic stability of sodium silicate gels in the presence of aluminum. J. Mater. Sci. 45, 5370–5377.

Hairi, S.N.M., Jameson, G.N., Rogers, J.J., MacKenzie, K.J., 2015. Synthesis and properties of inorganic polymers (geopolymers) derived from Bayer process residue (red mud) and bauxite. J. Mater. Sci. 50, 7713–7724.

Hajjaji, W., Pullar, R.C., Labrincha, J.A., Rocha, F., 2016. Aqueous Acid Orange 7 dye removal by clay and red mud mixes. Appl. Clay Sci. 126, 197–206.

Landi, E., Medri, V., Papa, E., Dedecek, J., Klein, P., Benito, P., Vaccari, A., 2013. Alkali-bonded ceramics with hierarchical tailored porosity. Appl. Clay Sci. 73, 56–64.

Liu, R.X., Poon, C.S., 2016. Effects of red mud on properties of self-compacting mortar. J. Clean. Prod. 135, 1170–1178.

Lloyd, R.R., Provis, J.L., Deventer, J.S.J., 2010. Pore solution composition and alkali diffusion in inorganic polymer cement. Cem. Concr. Res. 40, 1386–1392.

Novais, R.M., Buruberri, L.H., Ascensão, G., Seabra, M.P., Labrincha, J.A., 2016a. Porous biomass fly ash-based geopolymers with tailored thermal conductivity. J. Clean. Prod. 119, 99–107.

Novais, R.M., Ascensão, G., Seabra, M.P., Labrincha, J.A., 2016b. Waste glass from end-of-life fluorescent lamps as raw material in geopolymers. Waste Manag. 52, 245–255.

Novais, R.M., Ascensão, G., Buruberri, L.H., Senff, L., Labrincha, J.A., 2016c. Influence of blowing agent on the fresh-and hardened-state properties of lightweight geopolymers. Mater. Des. 108, 551–559.

Novais, R.M., Buruberri, L.H., Seabra, M.P., Bajare, D., Labrincha, J.A., 2016d. Novel porous fly ash-containing geopolymers for pH buffering applications. J. Clean. Prod. 124, 395–404.

Pérez-Villarejo, L., Corpas-Iglesias, F.A., Martínez-Martínez, S., Artiaga, R., Pascual-Cosp, J., 2012. Manufacturing new ceramic materials from clay and red mud derived from the aluminium industry. Constr. Build. Mater. 35, 656–665.

Pontikes, Y., Machiels, L., Onisei, S., Pandelaers, L., Geysen, D., Jones, P.T., Blanpain, B., 2013. Slags with a high Al and Fe content as precursors for inorganic polymers. Appl. Clay Sci. 73, 93–102.

Provis, J.L., Palomo, A., Shi, C., 2015. Advances in understanding alkali-activated materials. Cem. Concr. Res. 78, 110–125.

Ruģele, K., Bumanis, G., Bajare, D., Lakevičs, V., Rubulis, J., 2014. Alkaline activated material for pH control in biotechnologies. Key Eng. Mater. 604, 223–226.

Sahu, M.K., Mandal, S., Yadav, L.S., Dash, S.S., Patel, R.K., 2016. Equilibrium and kinetic studies of Cd (II) ion adsorption from aqueous solution by activated red mud. Desalination Water Treat. 57, 14251–14265.

Singh, M., Upadhayay, S.N., Prasad, P.M., 1996. Preparation of special cements from red mud. Waste Manag. 16, 665–670.

Škvára, F., Kopecký, L., Myšková, L., Šmilauer, V., Alberovska, L., Vinšová, L., 2009. Aluminosilicate polymers–influence of elevated temperatures, efflorescence. Ceram. –Silikáty 53, 276–282.

Taconi, K.A., Zappi, M.E., French, W.T., Brown, L.R., 2007. Feasibility of methanogenic digestion applied to a low pH acetic acid solution. Bioresour. Technol. 98, 1579–1585.

Wang, J.P., Chen, Y.Z., Ge, X.W., Yu, H.Q., 2007. Optimization of coagulation–-flocculation process for a paper-recycling wastewater treatment using response surface methodology. Colloid. Surf. A 302, 204–210.

World Population Prospects, 2015. The 2015 Revision. United Nations Department of Economic and Social Affairs/Population Division, New York, USA. esa.un.org/unpd/wpp/Publications/Files/Key_Findings_WPP_2015.pdf (Accessed 28 August 2016).

Zhang, Z., Wang, H., Provis, J.L., Bullen, F., Reid, A., Zhu, Y., 2012. Quantitative kinetic and structural analysis of geopolymers. Part 1. The activation of metakaolin with sodium hydroxide. Thermochim. Acta 539, 23–33.

Zhang, Z., Provis, J.L., Reid, A., Wang, H., 2014. Fly ash-based geopolymers: the relationship between composition, pore structure and efflorescence. Cem. Concr. Res. 64, 30–41.

Zhuang, X.Y., Chen, L., Komarneni, S., Zhou, C.H., Tong, D.S., Yang, H.M., Wang, H., 2016. Fly ash-based geopolymer: clean production, properties and applications. J. Clean. Prod. 125, 253–267.